Appl. Phys. B (2016) 122:224
DOI 10.1007/s00340-016-6505-x

Applied Physics B
Lasers and Optics

Spin-polarized lithium diffusion in a glass hot-vapor cell

Kiyoshi Ishikawa[1]

Received: 23 May 2016 / Accepted: 28 July 2016 / Published online: 2 August 2016

Abstract We report diffusion coefficients of optically pumped lithium atoms in helium buffer gas. The free-induction decay and the spin-echo signals of ground-state atoms were optically detected in an external magnetic field with the addition of field gradient. Lithium hot vapor was produced in a borosilicate-glass cell at a temperature between 290 and 360 °C. The simple setup using the glass cells enabled lithium atomic spectroscopy in a similar way to other alkali-metal atoms and study of the collisional properties of lithium atoms in a hot-vapor phase.

1 Introduction

Alkali-metal atoms in both hot and cold vapors have been intensively investigated in atomic physics. Precision measurements are performed by eliminating gradient of temperature, magnetic, and electric fields across the atomic vapor. The glass cells, consisting of nonmagnetic and nonmetallic transparent materials, are suited for uniform heating. An exception is lithium (Li) atoms, which have been studied mostly for hot vapor in the metal cells [1–5] and the glass gas-flow cells [6], and for atomic beam [7, 8] and cold atoms [9, 10]. The cells are heated at high temperatures (300–400 °C) to increase the Li vapor pressure. Since lithium is a mobile atom and penetrates into a variety of materials, the optical materials such as silicate and silica glasses, and even sapphire crystal have an attack of the Li atoms and take on a coloration. Therefore, only a few works were reported for hot Li vapor in the glass cells [11, 12], leading to a lack of information about collisional properties to other atoms and molecules [13]. To avoid the cell broken by direct contact with the liquid metal, the Li metal should be melted on a container in the glass cell. The crystals, MgO and CaF_2, are Li-metal resistant [3, 7] and can be nonmagnetic container compatible with the measurements of the spin coherence [14], nuclear-spin-polarized atomic probe [15], and conventional nuclear magnetic resonance [16]. In this work, the Li metal put into commercial MgO ceramic pot was sealed in the borosilicate-glass cells. Each cell was filled with the helium (He) buffer gas at a pressure of several kPa, or manufactured in vacuum. The diffusion coefficients of the optically pumped Li atoms were measured by optical detection of spin-echoes with variation of magnetic field gradient. Because the glass cells were uniformly heated, the measurements were feasible in the absence of convection and at a lower temperature than required in the metal cells. The spin polarization transport and the isotope effect of the smallest alkali-metal element, ^{6}Li and ^{7}Li, are studied in the ^{4}He gas.

2 Experiment

The Li vapor cells were manufactured in a similar procedure to other alkali-vapor cells [17]. Here, the outline is described and the details will be presented elsewhere. The ceramic MgO pots were baked in the borosilicate-glass cells at 400 °C until the residual pressure was $<5 \times 10^{-5}$ Pa. The glass manifold was filled with atmospheric pressure of He gas and uncoupled from the vacuum equipment. In a plastic bag filled with He gas, bulk Li metal of natural stable isotope ratio was trimmed and put into the ceramic pot in the glass cell. The manifold was evacuated again and baked

✉ Kiyoshi Ishikawa
ishikawa@sci.u-hyogo.ac.jp

[1] Graduate School of Material Science, University of Hyogo, Hyogo 678-1297, Japan

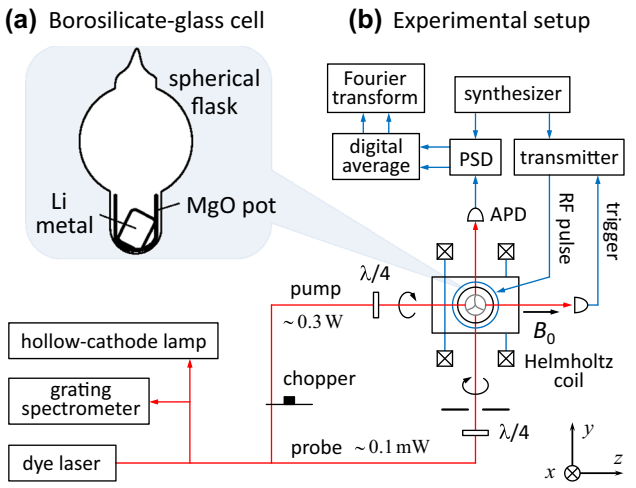

Fig. 1 **a** Side view of borosilicate-glass cell. The Li metal was placed in a MgO pot at the bottom of spherical cell (radius $R = 2.5$ cm). The metal did not directly contact with the glass wall. The vapor cells passed through many cycles between room temperature and 290 °C. **b** A single-mode dye laser was coarsely tuned by a grating spectrometer and achieved a resonance with the Li D lines by optogalvano signals using a hollow-cathode lamp. Pump laser pulse (duration 5 ms) was sent along z axis and probe beam along y axis. Both beams were circularly polarized and expanded in diameter. The static magnetic field $B_0 = 200\,\mu$T was applied along z axis. Magnetic field pulses oscillating along x axis were applied after optical pumping. The transient signals were phase-sensitively detected, averaged, and Fourier transformed. The coils for magnetic field cancelation and for gradient along z axis are not shown

at 350 °C for a few hours to achieve the pressure less than 5×10^{-5} Pa. After filled with He gas at a certain pressure $p_{\rm He}$ at room temperature $T_{\rm r} = 22\,^{\circ}$C, the glass cell was pulled off by flame sealing. In this work, the diffusion coefficient of Li atoms is reported for $p_{\rm He} = 8.3$ kPa, where the number density is $n_{\rm He} = p_{\rm He}/k_{\rm B}T_{\rm r} = 2.0 \times 10^{18}$ cm^{-3} and $k_{\rm B}$ is the Boltzmann constant. The finished cells were typically as shown in Fig. 1a.

The optical setup for atomic diffusion measurement is shown in Fig. 1b. The pump and the probe beams were circularly polarized from a single-mode dye laser tuned to the Li D lines at the wavelength of 671 nm. A static magnetic field, $B_0 = 200\,\mu$T, was applied along z axis, and the field along x and y axes was nulled as much as possible. The pump duration of 5 ms was large enough for spin polarization. At the end of optical pumping, pump transmission was increased at D_1 line and decreased at D_2 line. The ground-state hyperfine splittings, 228 MHz (^{6}Li, $I = 1$) and 803 MHz (^{7}Li, $I = 3/2$) [8], were less than the Doppler width of approximately 3 GHz (the mean thermal velocity $v_t = \sqrt{8k_{\rm B}T/\pi m_7} = 1300$ m/s, where m_7 is the mass of ^{7}Li atom). Because of the broad absorption line, only a part of atoms were pumped by the single-mode laser with no buffer gas. At low pressure, the hyperfine levels were pumped with the help of velocity-changing collisions with buffer gas. When pressure broadening became similar to the hyperfine splitting and then the Doppler width, hyperfine pumping was avoided and most of the Li atoms were optically polarized. In this work, the pressure broadened width was expected to be 1.5 GHz [6], sufficiently less than the fine-structure splitting of 10 GHz.

To avoid convection, the whole glass cell was heated at a temperature T uniformly in an oven. For a few hours at $T = 360\,^{\circ}$C, the glass body near bulk Li metal took on a dark-brown coloration, but the optical windows remained clean because they were far from the metal. When the cell was kept less than $T = 290\,^{\circ}$C, any coloration was not noticed for the cell body and the windows after optical experiment of a total of roughly 60-h heating time. The emission from the excited atoms was visible only above the bulk metal in a vacuum cell. These observations suggest that a net atom transfer was quasi-steady in the gas phase and the system was thermally non-equilibrated. That is, the metal was evaporated, the vapor atoms adsorbed on the walls, some atoms were thermally desorbed, and others were continuously absorbed in the glass material [18]. The motion process of each atom is locally a diffusion in the buffer gas. When atom desorption is negligible, distribution of dilute atoms n_i is non-uniform. A net transfer of atoms is described by the same coefficient as the local diffusion D_i ($i = 6$ for ^{6}Li, 7 for ^{7}Li). From Fick's law, the diffusion flux $\boldsymbol{J}_i$ is proportional to the density gradient, $\boldsymbol{J}_i = -D_i \nabla n_i$. By elementary theory,

$$D_i = v_t \ell_m / 3, \tag{1}$$

where the mean free path $\ell_m = t_m v_t$, the mean free time $t_m = 1/n_{\rm He} v_r \sigma$, the mean thermal relative velocity $v_r = \sqrt{8k_{\rm B}T/\pi\mu_i}$, and the reduced mass μ_i of colliding partners. Because of smallness of atomic mass and collision, cross-section σ, D_i can be one to two orders of magnitude larger than those of other alkali atoms [13].

The spin-polarized atoms worked as a tracer to measure the diffusion coefficient. The ground-state spin-echoes were induced by the radio frequency $\pi/2$ and the π pulses and detected by the probe transmission with the magnetic field gradient $G = \partial B_z/\partial z$. It is called continuous field gradient spin-echo method. The transient signals appeared able to be detected at $T = 220\,^{\circ}$C and were recorded at $T = 290\,^{\circ}$C. The signal amplitude was reasonable considering that lithium atom density was 7×10^9 cm^{-3} at thermal equilibrium of $T = 290\,^{\circ}$C, which is nearly equal to that of Rb vapor at room temperature [19]. The magnetic resonance frequencies were $\nu_6 = 1.9$ MHz (^{6}Li) and $\nu_7 = 1.4$ MHz (^{7}Li). Despite large frequency difference, the ^{6}Li signal by D_2 pumping was disturbed by an order of magnitude larger ^{7}Li signal by D_1 pumping because two absorption lines were overlapped within the Doppler

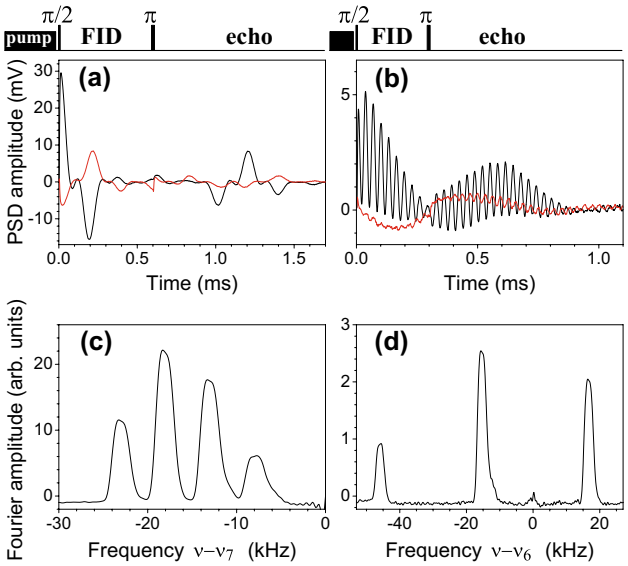

Fig. 2 Phase-sensitively detected free-induction decay and spin-echo signals for **a** ^{7}Li and **b** ^{6}Li atoms in ^{4}He gas at $T = 290\,^{\circ}\mathrm{C}, B_0 = 200\,\mu\mathrm{T}$ and $G = 0.1\,\mu\mathrm{T/cm}$. The radio frequency $\pi/2$ pulse (duration of 2.2 μs) was applied at $t = 0$ s and the π pulse (4.4 μs) at **a** $\tau = 600\,\mu\mathrm{s}$ and **b** 300 μs, as shown in top time sequence. Spin-echo was focused at 2τ. The in-phase (*black*) and the out-of-phase (*red*) components of transient signals were Fourier-transformed for **c** ^{7}Li and **d** ^{6}Li atoms. The synthesizer frequency was detuned from the center by 15 kHz for convenience to show the lines

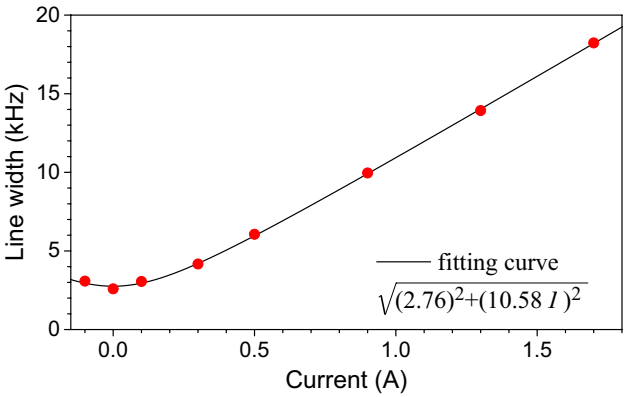

Fig. 3 Full width at half maximum w_{F} of Fourier spectral lines for the ^{6}Li atoms measured by changing the electric current of gradient coil. The residual width, 2.76 kHz, at the current of 0 A was due to fluctuating magnetic field

width. Therefore, the signals presented in this paper were measured via the respective D_1 lines with an isotope shift of 10 GHz. When atomic motion is described by a diffusion such that each step-length equals to mean free path, the echo amplitude at the echo time 2τ is expressed as [20, 21],

$$A(2\tau) = A_0 \exp\left(-2\gamma_i^2 G^2 \tau^3 D_i/3\right), \tag{2}$$

where γ_i is the gyromagnetic ratio. The amplitude A_0 was measured without intentional field gradient. Compared to the magnitude of B_0, field non-uniformity along x and y axes was negligible. Typically, 1024 traces were averaged for the ^{7}Li atoms and 4096 traces for the ^{6}Li atoms. The parameters were determined so that, without magnetic shield, the echo signals were not affected by ambient fluctuating magnetic field.

3 Result and discussion

Figure 2a and b shows the free-induction decay and the spin-echo signals of the ^{7}Li and the ^{6}Li atoms, respectively. The beat signals came from nonlinear Zeeman splitting due to small hyperfine splitting in the $2s\,^2S_{1/2}$ state. The spin exchange collisions between Li atoms were negligible in dilute vapor at $T = 290\,^{\circ}\mathrm{C}$. For dense atomic vapor, the decay time would be affected by the duration changes of the radio frequency and the light pulses [22, 23]. The decoherence of measured free-induction-decay signals was mainly due to atomic motion, non-uniform static magnetic field, and fluctuating field, as explained below. Due to large thermal velocity in a vacuum cell, the polarized atoms escaped from the probe beam during several cycles of spin precession. When transit time was increased with buffer gas, decoherence time was on the order of milliseconds. Therefore, dephasing of the signal from atoms at different places can be observed with the addition of magnetic field gradient. The external equipments produced time-varying magnetic field with the amplitude of the order of 0.1 μT, and the free-induction signals decayed by several hundred microseconds by averaging. Since the equipments were far from the cell, the fluctuating field was uniform within the cross-section of probe beam and the spin-echo signal was not canceled out by averaging. Therefore, the echo amplitude depended on the gradient G and the echo time 2τ, as shown in Eq. (2).

To estimate the gradient, the Fourier-transformed spectra were calculated from free-induction decay signals. As shown in Fig. 2c, d, the splitting of the ^{6}Li spectral lines was large enough to measure the line broadening by the gradient. Figure 3 shows that the line width w_{F} due to the gradient was expressed as $w_{\mathrm{F}}/I_{\mathrm{G}} = 10.58 \pm 0.04$ kHz/A, where I_{G} is the electric current of the gradient coil. The probe beam was shaped by a square through hole and the beam width w_{B} was 1.0 cm along z axis. Therefore, the magnetic field gradient was calibrated as $G/I_{\mathrm{G}} = 2\pi w_{\mathrm{F}}/\gamma_6 w_{\mathrm{B}} I_{\mathrm{G}} = 1.13\,\mu\mathrm{T/cm\,A}$. The overall spectral width of signals was mainly determined by nonlinear Zeeman splitting. It took a little wider by the field gradient, for example, 75 kHz for ^{6}Li and 30 kHz for ^{7}Li by applied maximum current $I_{\mathrm{G}} = 2$ A. Since the bandwidth of the π

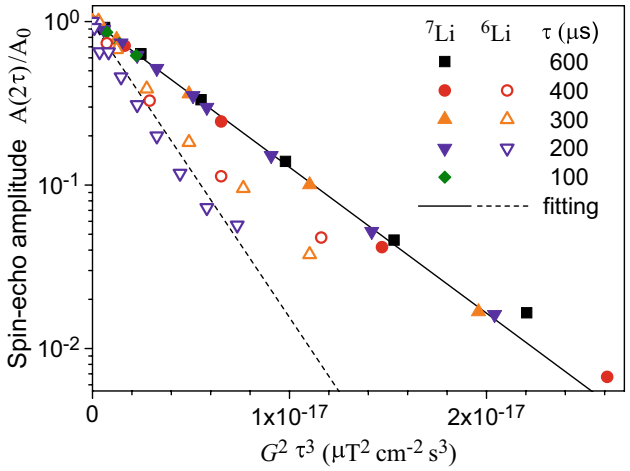

Fig. 4 Normalized spin-echo amplitude measured for the ^{7}Li (*closed marks*) and the ^{6}Li (*open marks*) atoms in He gas of $n_{\mathrm{He}} = 2.0 \times 10^{18}\,\mathrm{cm}^{-3}$ at $T = 290\,^{\circ}\mathrm{C}$. All the measured data were used in curve fitting for both isotopes. Because unnormalized amplitude was small for ^{6}Li, baseline noise disturbed fitting especially for large τ. The fitting errors were magnified for the small signals in the vertical logarithmic scale. The horizontal axis is scaled by magnetic field gradient G and half the echo time τ

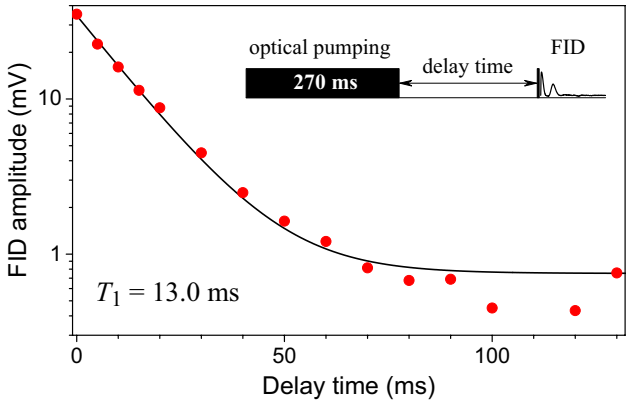

Fig. 5 Free-induction decay signals were delayed from optical pumping. The initial amplitude of the ^{7}Li signals decayed at $T_1 = 13.0$ ms for $n_{\mathrm{He}} = 2.0 \times 10^{18}\,\mathrm{cm}^{-3}$ and $T = 290\,^{\circ}\mathrm{C}$. The vertical axis is in logarithmic scale

pulse, 200 kHz, was sufficiently larger than signal spectral width, by tuning to the center of resonance lines, the spin tipping angle was not much dependent on the field gradient, assuring the use of Eq. (2).

Figure 4 shows the echo amplitude for the ^{7}Li and the ^{6}Li atoms. For several gradients and echo times, the measured amplitudes were sufficiently fitted by a single exponential curve in Eq. (2). Therefore, atomic motion can be described by normal diffusion. Neither anomalous diffusion such as Lévy flight nor convection was necessary to consider in this measurement. The diffusion coefficients of Li atoms were $D_7 = 140.6 \pm 1.5\,\mathrm{cm}^2/\mathrm{s}$ and $D_6 = 160 \pm 13\,\mathrm{cm}^2/\mathrm{s}$. The ratio $D_6/D_7 = 1.138 \pm 0.092$ was consistent with the calculated value, 1.133, by the elementary theory on Eq. (1). Therefore, the difference in diffusion coefficient came from mass difference of lithium isotopes. From Eq. (1), the mean free paths, $\ell_{m7} = 32.36 \pm 0.35\,\mu\mathrm{m}$ and $\ell_{m6} = 34.1 \pm 2.7\,\mu$m, were much smaller than the laser beam and the cell dimensions. The mean free times, $t_{7m} = 24.8 \pm 0.3$ ns and $t_{6m} = 24 \pm 2$ ns, were much smaller than the echo time. These results assure the statistical consistency of the measurement. In future work on spin polarization flow to the walls, even in the presence of buffer gas, ballistic motion of the Li atoms should be taken into account within the mean free path from the walls.

According to Eq. (1), the diffusion coefficient depends on the number density of buffer gas n and the temperature T, as follows,

$$D = D_0 \frac{\sqrt{T}/n}{\sqrt{T_0}/n_0}, \tag{3}$$

where D_0 is the value of the diffusion coefficient at a reference temperature T_0, and at a reference number density n_0. These are taken to be the number density of an ideal gas at a pressure of 1 atm and a temperature of 0 °C($n_0 = 2.69 \times 10^{19}\,\mathrm{cm}^{-3}$). Here, the coefficients are compared between different alkali-metal atoms: $D_0 = 7.43\,\mathrm{cm}^2/\mathrm{s}$ for the ^{7}Li atoms in ^{4}He gas is much larger than $D_0 = 0.31\,\mathrm{cm}^2/\mathrm{s}$ for the ^{133}Cs atoms in ^{4}He gas [24] and $D_0 = 0.118\,\mathrm{cm}^2/\mathrm{s}$ for the ^{85}Rb atoms in nitrogen gas [21].

During long period of optical pumping, 270 ms, quasi-steady distribution of the polarized atoms was achieved in the cell. After optical pumping, the polarization was relaxed until the delayed $\pi/2$ pulse was applied. As shown in Fig. 5, the initial amplitude of free-induction signal decayed with the time constant $T_1 = 13.0 \pm 0.4$ ms. Since the fine splitting in the lowest excited state is smaller than those of other alkali atoms, spin relaxation in the ground state should be negligible by collisions to He gas of the current pressure [25]. With no specific anti-relaxation coating on the glass surface, the polarization was decayed by single collisions to the walls. When atom density was uniform in the cell, the decay time due to the wall relaxation would be $(R/\pi)^2/D_i = 4.5$ ms for the slowest diffusion mode in a spherical cell [26]. A possible explanation for apparent slow relaxation of $T_1 > 4.5$ ms is that the atoms were absorbed in the glass and unpolarized atoms were not supplied by desorption from the walls. Even in the relatively large cell, therefore, the spin angular momentum can be sufficiently transferred by the Li atoms from the vapor

phase to the walls. For more details on diffusion spin currents in gas phase, it is necessary to study the collisional properties of Li atoms in the buffer gas, such as *S*-damping and hyperfine shift collisions in the ground state, and *J*-damping and fine-structure changing collisions in the excited state [13, 27].

4 Summary

The diffusion coefficients and the isotope effect of spin-polarized lithium atoms were measured in helium gas. The borosilicate-glass vapor cells were compatible with optical and magnetic resonance experiments and available in many temperature cycles. The temperature of 290 °C was high enough to produce vapor density for optical measurement, and no coloration was found on the windows and the cell body. The windows remained clean when the glass near bulk metal took on a coloration at high temperatures. Due to absorption into glass materials, atomic flow was directed from evaporating bulk metal to the walls via gas phase. When spin exchange collisions were negligible in dilute atomic vapor, the flux of angular momentum was described by diffusion equation of atoms. Since the measured diffusion coefficient was much larger than those of other alkali-metal atoms, the fast transfer of atoms and angular momenta is expected in the gas. To evaluate spin polarization currents accurately, it is important to measure the collisional properties of lithium atoms in various buffer gases.

Acknowledgments This work was supported in part by JSPS KAKENHI Grant Numbers 25610115 and 16H04030. KI acknowledges N. Hamada for setup of lithium optogalvano saturation spectroscopy.

References

1. C.R. Vidal, J. Cooper, Heat-pipe oven: a new, well-defined metal vapor device for spectroscopic measurements. J. Appl. Phys. **40**(8), 3370–3374 (1969)
2. P. Minguzzi, F. Strumia, P. Violino, Optical pumping of lithium vapour. Opt. Commun. **1**(1), 1–2 (1969)
3. V.J. Slabinski, R.L. Smith, Lithium vapor cell and discharge lamp using MgO windows. Rev. Sci. Instrum. **42**(9), 1334–1338 (1971)
4. I.E. Olivares, A.E. Duarte, T. Lokajczyk, A. Dinklage, F.J. Duarte, Doppler-free spectroscopy and collisional studies with tunable diode lasers of lithium isotopes in a heat-pipe oven. J. Opt. Soc. Am. B **15**(7), 1932–1939 (1998)
5. D. Sun, C. Zhou, L. Zhou, J. Wang, M. Zhan, Modulation transfer spectroscopy in a lithium atomic vapor cell. Opt. Express **24**(10), 10649–10662 (2016)
6. A. Gallagher, Noble-gas broadening of the Li resonance line. Phys. Rev. A **12**, 133–138 (1975)
7. K.C. Brog, T.G. Eck, H. Wieder, Fine and hyperfine structure of the 2^2p term of Li^6 and Li^7. Phys. Rev. **153**, 91–103 (1967)
8. C.J. Sansonetti, C.E. Simien, J.D. Gillaspy, J.N. Tan, S.M. Brewer, R.C. Brown, S. Wu, J.V. Porto, Absolute transition frequencies and quantum interference in a frequency comb based measurement of the ^{6,7}LiD lines. Phys. Rev. Lett. **107**, 023001 (2011)
9. M. Taglieber, A.-C. Voigt, T. Aoki, T.W. Hänsch, K. Dieckmann, Quantum degenerate two-species fermi-fermi mixture coexisting with a bose-einstein condensate. Phys. Rev. Lett. **100**, 010401 (2008)
10. S. Brakhane, W. Alt, D. Meschede, C. Robens, G. Moon, A. Alberti, Note: ultra-low birefringence dodecagonal vacuum glass cell. Rev. Sci. Instrum. **86**(12), 126108 (2015)
11. J.J. Wright, L.C. Balling, R.H. Lambert, Hyperfine splittings and pressure shifts of Li^6 and Li^7. Phys. Rev. **183**, 180–185 (1969)
12. S .N. Atutov, B .V. Bondarev, S .M. Kobtzev, P .V. Kolinko, S .P. Podjachev, A .M. Shalagin, Light-induced diffusive pulling (pushing) of lithium atoms into a laser beam. Measurement of diffusion coefficients of lithium in 2p and 2s states in noble gases. Opt. Commun. **115**((3–4)), 276–282 (1995)
13. W. Happer, Y.-Y. Jau, T.G. Walker, *Optically Pumped Atoms* (Wiley, Weinheim, 2010)
14. D. Budker, M. Romalis, Optical magnetometry. Nat. Phys. **3**(4), 227–234 (2007)
15. R.F. Haglund, D. Fick, B. Horn, E. Koch, Spin-polarized nuclei as probes of electromagnetic field distributions on solid surfaces. Hyperfine Interact. **30**(2), 73–108 (1986)
16. K. Ishikawa, Spin-injection optical pumping of molten cesium salt and its NMR diagnosis. AIP Adv. **5**(7), 077122 (2015)
17. B. Patton, K. Ishikawa, Y.-Y. Jau, W. Happer, Intrinsic impurities in glass alkali-vapor cells. Phys. Rev. Lett. **99**(2), 027601 (2007)
18. J. Ma, A. Kishinevski, Y.-Y. Jau, C. Reuter, W. Happer, Modification of glass cell walls by rubidium vapor. Phys. Rev. A **79**, 042905 (2009)
19. A.N. Nesmeyanov, *Vapor pressure of the chemical elements* (North-Holland, Amsterdam, 1963)
20. P.T. Callaghan, *Principles of nuclear magnetic resonance microscopy* (Clarendon, Oxford, UK, 1991)
21. K. Ishikawa, T. Yabuzaki, Diffusion coefficient and sublevel coherence of Rb atoms in N_2 buffer gas. Phys. Rev. A **62**, 065401 (2000)
22. S. Appelt, A.B. Baranga, A.R. Young, W. Happer, Light narrowing of rubidium magnetic-resonance lines in high-pressure optical-pumping cells. Phys. Rev. A **59**, 2078–2084 (1999)
23. K. Ishikawa, T. Kojima, T. Hasegawa, Y. Takagi, Spin dynamics of dense alkali-metal atoms. Phys. Rev. A **65**, 032511 (2002)
24. K. Ishikawa, Y. Anraku, Y. Takahashi, T. Yabuzaki, Optical magnetic-resonance imaging of laser-polarized Cs atoms. J. Opt. Soc. Am. B **16**(1), 31–37 (1999)
25. T.G. Walker, J.H. Thywissen, W. Happer, Spin-rotation interaction of alkali-metal-He-atom pairs. Phys. Rev. A **56**, 2090–2094 (1997)
26. F.A. Franz, E. Lüscher, Spin relaxation of optically pumped cesium. Phys. Rev. **135**, A582–A588 (1964)
27. K. Ishikawa, B. Patton, B.A. Olsen, Y.-Y. Jau, W. Happer, Transfer of spin angular momentum from Cs vapor to nearby Cs salts through laser-induced spin currents. Phys. Rev. A **83**(6), 063410 (2011)